Anal. Chem. **2005,** *77,* 6989−6998

Development of a Cryogen-Free Concentration System for Measurements of Volatile Organic Compounds

Barkley C. Sive,*,† Yong Zhou,† Donald Troop,† Yuanli Wang,† William C. Little,‡ Oliver W. Wingenter,§ Rachel S. Russo,† Ruth K. Varner,† and Robert Talbot†

Climate Change Research Center, Institute for the Study of Earth, Oceans, and Space, University of New Hampshire, Durham, New Hampshire 03824, MMR Technologies, Inc., 1400 North Shoreline Boulevard, Suite A5, Mountain View, California 94043-1346, and Department of Chemistry, New Mexico Institute of Mining and Technology, Socorro, New Mexico 87801

An innovative cryogen-free concentrator system for measurement of atmospheric trace gases at the parts per trillion level has been developed with detection by routinely used gas chromatographic methods. The first-generation system was capable of reaching a trapping temperature of −186 °C, while the current version can reach −195 °C. A Kleemenko cooler is used to create liquid nitrogen equivalent trapping conditions and eliminate the use of solid absorbents, a potential source of artifacts. The method utilizes dual-stage trapping with individual cold regions. The two stages are cooled to −20 and −175 °C for water management and sample enrichment, respectively. Both stages house a Silonite-coated stainless steel sample loop; the second stage loop is filled with 1-mm-diameter glass beads, which provide an inert surface area for analyte concentration. In our application, the complete system employed four channels utilizing two flame ionization detectors, one electron capture detector, and a mass spectrometer. The system was automated for unattended operation and was deployed off the New England east coast on Appledore Island to measure a suite of ambient non-methane hydrocarbons, halocarbons, alkyl nitrates, and oxygenated volatile organic compounds during the International Consortium for Atmospheric Research on Transport and Transformation field campaign in summer 2004. This robust system quantified 98 ambient volatile organic compounds with precisions ranging from 0.3 to 15%.

Volatile organic compounds (VOCs; include non-methane hydrocarbons, oxygenated hydrocarbons, halocarbons, and alkyl nitrates) play key roles in the chemistry of the atmosphere[1,2] and have a number of anthropogenic and natural sources.[3,4] Oxidation of non-methane hydrocarbons (NMHCs) produces a suite of free radicals that are involved in NO_x ($NO + NO_2$)-catalyzed reactions, which generate ozone (O_3) in the troposphere.[5,6] Subsequent photodissociation of O_3 by UV light (<320 nm) produces excited-state oxygen, $O(^1D)$, which can react with water vapor to form hydroxyl radical (HO), the chief oxidant for most VOCs.[7] This reaction channel is the primary source of HO, especially in the lower troposphere. Other HO channels involving oxygenated VOCs (OVOCs) become increasingly important at higher altitudes in the troposphere.[8,9]

Anthropogenic and natural halocarbons are well known as stratospheric ozone-depleting compounds. Specific hydrocarbons and halocarbons are useful as tracers to identify emission source inputs to air masses.[10] For example, tetrachlorethene and trichloroethene are used as urban/industrial tracers, while bromoform reflects influence from the marine environment. In addition to providing information on sources, the VOC mixture in an air mass

* Corresponding author. Phone: (603) 862-3132. Fax: (603) 862-2124. E-mail: bcs@ccrc.sr.unh.edu.

† University of New Hampshire.

‡ MMR Technologies, Inc.

§ New Mexico Institute of Mining and Technology.

(1) Thompson, A. M. *Science* **1992**, *256*, 1157−1168.

(2) Wang, Y.; Jacob, D. J.; Logan, J. A. *J. Geophys. Res.* **1998**, *103*, 10757−10768.

(3) Guenther, A.; Hewitt, C. N.; Erickson, D.; Fall, R.; Geron, C.; Graedel, T.; Harley, P.; Klinger, L.; Lerdau, M.; McKay, W. A.; Pierce, T.; Scholes, B.; Steinbrecher, R.; Tallamraju, R.; Talor, J.; Zimmerman, P. *J. Geophys. Res.* **1995**, *100*, 8873−8892.

(4) Keene, W. C.; Khalil, M. A. K.; Erickson, D. J.; McCulloch, A.; Graedel, T. E.; Lobert, J. M.; Aucott, M. L.; Gong, S. L.; Harper, D. B.; Kleiman, G.; Midgley, P.; Moore, R. M.; Seuzaret, C.; Sturges, W. T.; Benkovitz, C. M.; Koropalov, V.; Barrie, L. A.; Li, Y. F. *J. Geophys. Res.* **1999**, *104*, 8429−8440.

(5) McKeen, S. A.; Hsie, E. Y.; Trainer, M.; Tallamraju, R.; Liu, S. C. *J. Geophys. Res.* **1991**, *96*, 10809−10846.

(6) Riemer, D. D.; Pos, W.; Milne, P.; Farmer, C.; Zika, R.; Apel, E.; Olszyna, K.; Kliendienst, T.; Lonneman, W.; Bertman, S.; Shepson, P.; Starn, T. *J. Geophys. Res.* **1998**, *103*, 28111−28128.

(7) Davis, D. D.; Chen, G.; Crawford, J. H.; Liu, S.; Tan, D.; Sandholm, S. T.; Jing, P.; Cunnold, D. M.; DiNunno, B.; Browell, E. V.; Grant, W. B.; Fenn, M. A.; Anderson, B. E.; Barrick, J. D.; Sachse, G. W.; Vay, S. A.; Hudgins, C. H.; Avery, M. A.; Lefer, B.; Shetter, R. E.; Heikes, B. G.; Blake, D. R.; Blake, N. J.; Kondo, Y.; Oltmans, S. *J. Geophys. Res.* **2003**, *108*, 8829−8847.

(8) Prather, M. J.; Jacob, D. J. *Geophys. Res. Lett.* **1997**, *24*, 3189−3192.

(9) Crawford, J.; Davis, D.; Olson, J.; Chen, G.; Liu, S.; Gregory, G.; Barrick, J.; Sachse, G.; Sandholm, S.; Heikes, B.; Singh, H.; Blake, D. *J. Geophys. Res.* **1999**, *104*, 16255−16273.

(10) Blake, N. J.; Blake, D. R.; Wingenter, O. W.; Sive, B. C.; McKenzie, L. M.; Lopez, J. P.; Simpson, I. J.; Fuelberg, H. E.; Sachse, G. W.; Anderson, B. E.; Gregory, G. L.; Carroll, M. A.; Albercook, G. M.; Rowland, F. S. *J. Geophys. Res.* **1999**, *104*, 16213−16232.

10.1021/ac0506231 CCC: $30.25
Published on Web 09/23/2005

provides general clues on the extent of its photochemical aging and mixing processes.[11−19] This is made possible by the differential reactivity and lifetimes of hydrocarbons and halocarbons, which vary from minutes to decades. These differences have also been exploited to identify and quantify the presence of oxidants such as atomic Cl and Br.[12−14]

As part of our ongoing commitment to improve the analytical capabilities of AIRMAP (http://airmap.unh.edu/), a University of New Hampshire (UNH) air quality and climate program, we have recently made significant improvements and advances in the measurement of atmospheric VOCs to facilitate long-term monitoring at remote locations. Most current techniques for measurements of VOCs involve the use of liquid cryogen, beginning with a sample concentration step using liquid nitrogen, followed by rapid heating of the sample loop, and detection by standard gas chromatographic methods. Manual operations can be tedious, particularly when employed at field locations, and are complicated greatly by the use and availability of large volumes of liquid nitrogen. In contrast to manual operations, many automated instruments deployed remotely for atmospheric trace gas measurements rely on the use of solid adsorbents, such as Tenax or Carbotrap, for sample concentration when liquid nitrogen is not readily available.[6,20,21] Although solid adsorbents have been proven reliable for concentrating certain atmospheric trace gases when the system is well characterized, there can be significant problems with artifacts during the sample enrichment and desorbtion processes.[22] This is particularly important when measuring trace gases such as methyl bromide and methyl iodide, with average atmospheric mixing ratios on the order of 10 and 0.5 pptv, respectively. Because small changes in mixing ratios can imply significant differences in sources when interpreting the final data, it is critical that VOC measurements reflect the true atmospheric composition. To alleviate problems with sample artifacts or augmentation, the system described here is capable of rapidly cooling a glass bead-filled loop for sample concentration, greatly reducing inadvertent chemical alteration of authentic aliquots of ambient air.

In this paper, we first describe an alternative method to using liquid cryogens for sample concentration of atmospheric VOCs. Second, results from this system are compared with ambient measurements conducted concurrently at Appledore Island, ME, with (1) real-time VOC measurements using a proton-transfer reaction mass spectrometer (PTR-MS) and (2) whole air samples collected in inert stainless steel electropolished canisters. The latter were analyzed at UNH using a traditional manual liquid nitrogen cryogenic trapping technique coupled with gas chromatographic analysis employing two flame ionization detectors (FIDs), two electron capture detectors (ECDs), and a mass spectrometer (MS). Overall, this new cryogen-free system offers superior performance with extremely high sensitivities and selectivity for atmospheric trace gas measurements.

EXPERIMENTAL SECTION

Cooling Unit. In collaboration with MMR Technologies (Mountain View, CA), the model CC2202 Cryofocus System was developed for the trapping of atmospheric trace gases at cryogenic temperatures and thermal desorption for their subsequent quantification by various methods with the only requirement being 350 W of electrical power to operate the cooler. The heart of the system is a Kleemenko cycle cooler that utilizes a multicomponent mixed refrigerant, in a single-stream, cascade, throttle-expansion refrigeration cycle.[23] The system is closely related to the refrigeration system of a home refrigerator but uses a different refrigerant capable of cooling to −200 °C. In the cycle, the compressed refrigerant is precooled in a countercurrent heat exchanger, where it liquefies. The liquid then passes through a capillary or throttling valve, dropping to a lower pressure, and evaporates such that the resulting cooled vapor precools the incoming high-pressure fluid. A standard, low-cost, commercially available oil-lubricated refrigeration compressor is the core of the Kleemenko cooler. The compressor has a typical operating life in excess of 100 000 h in normal operation. The other components of the system include a heat exchanger, condenser, oil separator, and evaporator.

The cooling system has two stages that can be operated independently, with each designed for rapid cycling using a single compressor. A significant advantage of this system compared to that described by von Hobe et al.[21] is that there are two individual cold regions, and each is equipped with an individual sample loop contained in a separate stainless steel dewar with a removable lid. The interiors of the dewars are maintained at ambient atmospheric pressure in contrast to the von Hobe et al.[21] system, which requires a turbomolecular pump to maintain a pressure of $<10^{-4}$ h Pa for the system to cool to cryogenic temperatures. Air may pass in and out of the dewars during heating and cooling, but moisture is excluded by an ancillary drying column attached to the lid. The first cooling stage is housed in the smaller of two dewars, with the second stage in the larger one. Each dewar has its own temperature control for the associated sample loop and a coaxial refrigerant line carrying the high-pressure refrigerant and return vapor connects to a heat exchanger in each of the dewars. The flow through these lines is controlled by electronically actuated solenoid valves.

Relatively large volumes of ambient air need to be sampled to obtain limits of detection in the low pptv range for atmospheric VOCs. The purpose of the first stage is water management, which

(11) McKeen, S. A.; Liu, S. C. *Geophys. Res. Lett.* **1993**, *20*, 2363−2366.
(12) Wingenter, O. W.; Kubo, M. K.; Blake, N. J.; Smith, T. W., Jr.; Blake, D. R.; Rowland, F. S. *J. Geophys. Res.* **1996**, *101*, 4331−4340.
(13) Wingenter, O. W.; Blake, D. R.; Blake, N. J.; Sive, B. C.; Atlas, E.; Flocke, F.; Rowland, F. S. *J. Geophys. Res.* **1999**, *104*, 21819−21828.
(14) Jobson, B. T.; Niki, H.; Yokouchi, Y.; Bottenheim, J.; Hopper, F.; Leatich, R. *J. Geophys. Res.* **1994**, *99*, 25355−25368.
(15) Bertman, S. B.; Roberts, J. M.; Parrish, D. D.; Buhr, M. P.; Goldan, P. D.; Kuster, W. C.; Fehsenfeld, F. C.; Montzka, S. A.; Westberg, H. *J. Geophys. Res.* **1995**, *100*, 22805−22813.
(16) Flocke, F.; Volz-Thomas, A.; Buers, H.-J.; Pätz, W.; Garthe, H.-J.; Kley, D. *J. Geophys. Res.* **1998**, *103*, 5729−5746.
(17) Roberts, J. B.; Bertman, S. B.; Parrish, D. D.; Fehsenfeld, F. C. *J. Geophys. Res.* **1998**, *103*, 13569−13580.
(18) Stroud, C. A.; et al. *J. Geophys. Res.* **2001**, *106*, 23043−23053.
(19) Simpson, I. J.; Blake, N. J.; Blake, D. R.; Atlas, E.; Flocke, F.; Crawford, J. H.; Fuelberg, H. E.; Kiley, C. M.; Meinardi, S.; Rowland, F. S. *J. Geophys. Res.* **2003**, *108* (D20), 8808 (doi: 10.1029/2002JD002830).
(20) Lamanna, M. S.; Goldstein, A. H. *J. Geophys. Res.* **1999**, *104* (D17), 21247−21262.
(21) von Hobe, M.; Kenntner, T.; Helleis, F. H.; Sandovol-Soto, L.; Andreae, M. O. *Anal. Chem.* **2000**, *72*, 5513−5515.
(22) Apel, E. C.; Calvert, J. G.; Gilpin, T. M.; Fehsenfeld, F.; Lonneman, W. A. *J. Geophys. Res.* **2003**, *108* (D9), 4300 (doi: 10.1029/2002JD002936).
(23) Little, W. A. In *Proceedings from the Seventeenth International Cryogenic Engineering Conference*, Bournemouth, U.K.; Dew-Hughes, D., Scurlock, R. G., Watson, J. H. P., Eds.; Institute of Physics Publishing: Bristol, 1998; pp 1−9.

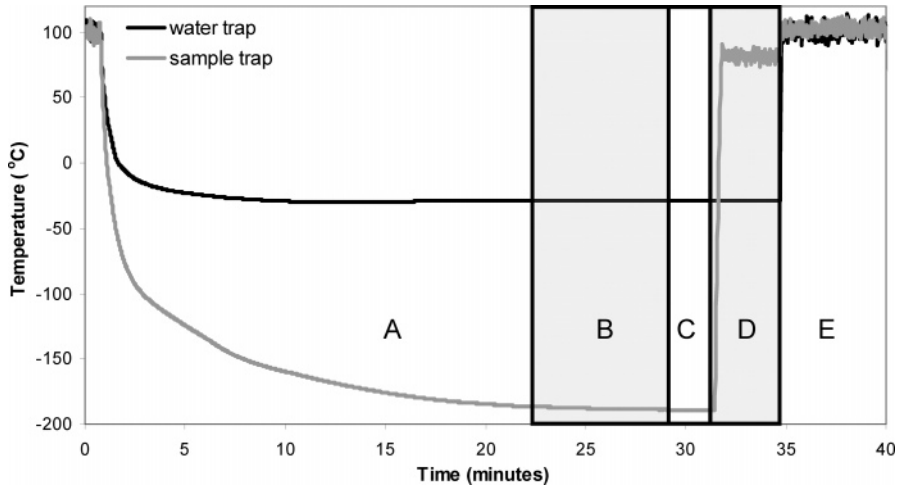

Figure 1. Cooling and heating cycles of the water management and sample enrichment loops. Regions: (A) is the cooling to the initial set points, (B) is the sample preflush and trap, (C) is the helium preflush and sweep, (D) is the desorb and inject, and (E) is the bakeout and helium purge.

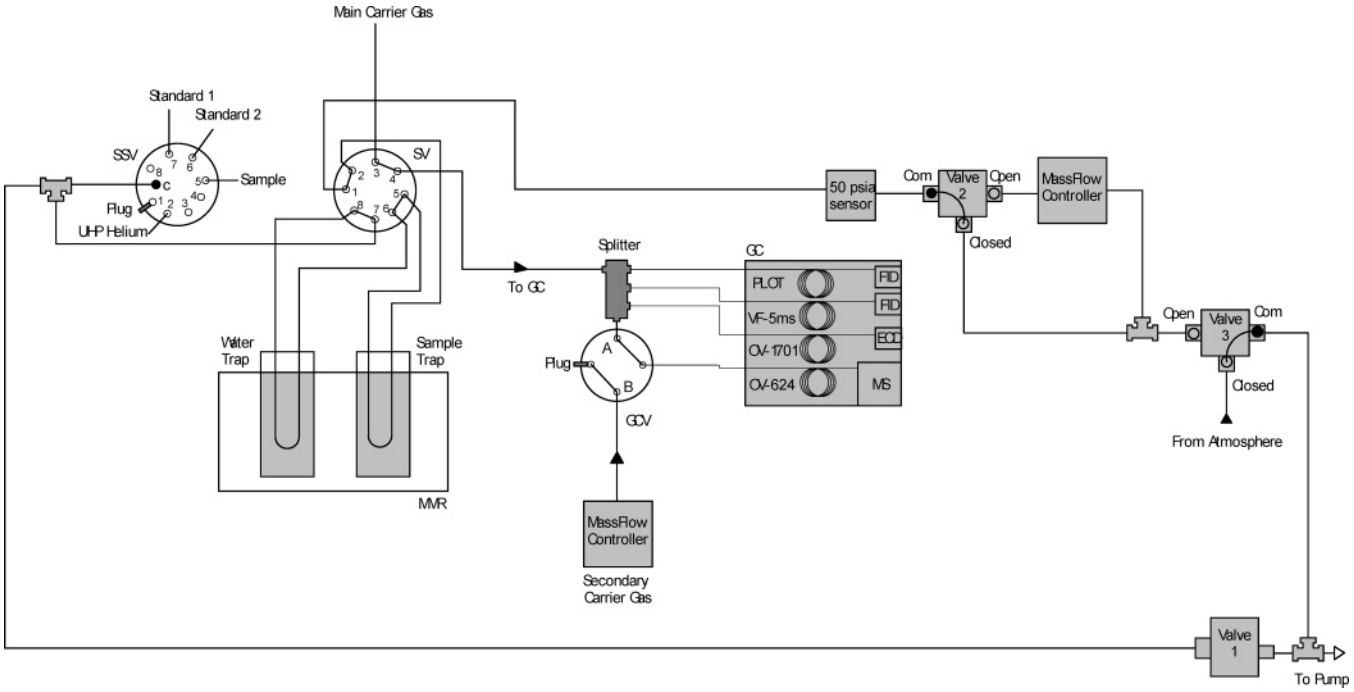

Figure 2. Schematic of the concentrator system and GC configuration.

is critically important in any cryogenic system that samples ambient air in the lower troposphere. The first stage was cooled to −20 °C for water management, but is capable of reaching temperatures down to −60 °C, while the second stage was cooled to −175 °C for sample enrichment. The system we deployed in the field during the summer of 2004 was capable of reaching −186 °C, but for faster sample throughput, it was only cooled to −175 °C. Both of the loop assemblies housed in each dewar were made of a 20 cm × 0.3175 cm Silonite-coated (Entech Instruments, Inc., Simi Valley, CA) stainless steel sample loop. The sample enrichment loop was filled with 1-mm-diameter glass beads (Ohio Valley, Marietta, OH) to provide an inert clean surface area for sample concentration. The sample loops were wrapped in 0.254-mm polyimide-coated nicrome wire (California Fine Wire, Grover Beach, CA) and affixed to a 0.56 o.d. (0.47 cm i.d.) × 14 cm long aluminum tube, which slides over and mates with a vertical and sealed refrigerant line (the cooling rod). A thermocouple is attached to the bottom of the loop to monitor its temperature independent of the cooling rod. The sample loop, aluminum tube, thermocouple, and heating wire are all wrapped in copper foil radiation shield, making the entire loop assembly easily removable from the dewar. Silicone rubber cement is used to seal the lid to the dewar to help keep moisture out of the interior. Both stages can be run independently of each other; e.g., one stage can be cooling while the other is heating, making the system extremely versatile. Typical cooling and heating cycles are shown in Figure 1 for the water management and sample enrichment dewars. For the instrument that was deployed in the summer of 2004, the cooling time from 100 to −175 °C was ∼22 min. After the system reached its initial set point of −175 °C, the sample trapping cycle began.

Sample Traps. A schematic of the concentration system is depicted in Figure 2, which consisted of an eight-port stream select valve (SSV) (Valco Instruments, Houston, TX), an eight-port switching valve (SV) (Valco Instruments), both containing Valcon E rotors and having $^1/_{16}$-in. ports, one two-way valve (valve 1, preflush control), two three-way valves (valves 2 and 3, MFC and pump control), a 50 psia pressure sensor, a Unit Instruments 8100 MFC (Yorba Linda, CA), and 0.3175-cm traps for water management and sample enrichment. The flow and switching pathways for the water management and sample enrichment loops is shown in Figure 2. The SSV is used to direct either ambient air or standards to the cooling unit for the sample enrichment process. The example depicted illustrates the "trapping mode," where the sample is first pulled through the water management loop and then the sample enrichment loop. All tubing is heated to 50 °C while the SSV and SV bodies are heated to 45 °C to prevent condensation and minimize memory effects.

The trapping procedure is initiated when the water management and sample enrichment loops reach their initial set point temperatures. When either a sample or standard is selected for analysis with the SSV, the lines are first preflushed for 10 s by opening valve 1, which pulls the air using a downstream diaphragm pump (Vacuubrand ME 2, Wertheim, Germany) through the SSV via the tee adjacent to it, bypassing the sample loops. After the preflush, valve 1 is closed and valves 2 and 3 are opened, redirecting the air flow to the SV where it passes through both loops at a rate of 200 cm^3 min^{-1} as maintained by a downstream mass flow controller. To minimize artifacts,[24] the flow of ambient air is only exposed to inert Silicosteel tubing with the exception of the Teflon valve assembly on the upstream metal bellows pump, which is used to keep the sample lines at a positive pressure, and the Valcon E rotors (a polyaryletherketone composite) in the SSV and SV. After the air sample trapping procedure is completed, valves 2 and 3 are closed and the SSV switched flow paths to the UHP helium for a helium sweep of the water and sample enrichment traps. The helium is preflushed for 10 s by opening valve 1 prior to directing the flow through the water management and sample enrichment traps. Analogous to the sample trapping procedure, valves 2 and 3 are then opened and 100 cm^3 of helium is pulled through both loops by the downstream pump and flow controller at a rate of 100 cm^3 min^{-1}. After the helium sweep is completed, the SSV is moved to position 1, which is a dead end flow path, and valves 1, 2, and 3 are all closed, isolating the water management and sample enrichment loops. After the loops are isolated, the sample enrichment trap is rapidly heated to 80 °C using 0.254-mm polyimide-coated nicrome wire, the SV is moved from "trap" to "inject", and the gas chromatograph (GC) is triggered to start the temperature program. Helium carrier gas flushes the contents of the sample enrichment loop through a 0.74-mm Silonite-coated heated transfer line to the splitter box.

Traps for CO_2, H_2O vapor, and O_3 removal are not used to minimize the possibility of artifacts in trace level measurements. We have found that an empty 0.3175-cm loop at −20 °C is adequate for water management during the sample trapping procedure. Even during periods of extremely high ambient humidity, ice blockage does not occur in the loops with samples sizes of 1500−2000 cm^3. For ozone removal, 100 cm^3 of UHP helium is passed through both sample loops at a rate of 100 cm^3 min^{-1} to alleviate ozone−alkene reactions when the second-stage loop is heated for sample desorption. Numerous experiments have been conducted in our laboratory, as well as others (E. Apel, NCAR and D. Riemer, University of Miami, personal communication, 2003), that demonstrate that this is a reliable way to quench ozone−alkene reactions for this type of system. Passing the sample stream through O_3 scrubbers, such as granular KI or crystalline Na_2SO_3, can be prone to artifacts and also requires regular maintenance.[25,26] Finally, CO_2 is not removed from the sample using an Ascarite trap since we have found that this too is prone to artifacts and is problematic for compounds other than light hydrocarbons. Instead, the CO_2 is trapped in the sample enrichment loop and injected on to each channel of the system. Since the electron capture and flame ionization detectors are blind to CO_2, there is no performance effect on these three channels. With the mass spectrometer, we do not use selected ion monitoring windows associated with CO_2 or its isotopes, but this does not negatively impact the suite of gases that can be measured with the system. However, because we are injecting water vapor and a large amount of CO_2 into the mass spectrometer, a decrease in multiplier response is observed, but only slightly more rapid than if dry samples without CO_2 are injected. Additionally, there is a "warm-up" period (~24 h) for the system to equilibrate to the CO_2 and water vapor that is injected on to each column and detector. Once the system has equilibrated, we see an improvement in the overall measurement precision of a few percent, depending on the trace gas and its mixing ratio in the atmosphere.

Instrument Control. The primary control hardware for the system is a personal computer (PC) running Windows XP with a National Instruments PCI-1200 data acquisition and control card. The PC controls the cooling and heating of the two dewars through an RS-232 port, while control of the SSV and SV are through a second RS-232 port. Other components, including the mass flow controller and valves 1−3, are controlled by the PCI-1200 card through a custom-designed circuit that was housed in the control/valve box to serve as a breakout for the PCI-1200 and provide power distribution to the valves. An additional four-port switching valve (used to control the secondary carrier flow for the MS, described below) is controlled by a personal measurement device (PMD) (PMD-1024LS, Measurement Computing Corp., Middleboro, MA) using a digital line; the PMD is connected to the PC through a USB port. The control/user interface program is written in National Instrument LabVIEW software. The AIRMAP concentrator program consists of one main virtual instrument (VI) and over a dozen sub-VIs. The program implements a finite state machine, which monitors and controls the temperature in two dewers, valve positions, and also triggers the GC. One complete cycle consists of eight software states from the initial cool state to the final bakeout state. The cooling and heating cycles of the water management and sample enrichment loops depicted as the

(24) Apel, E. C.; Hills, A. J.; Leub, R.; Zindel, S.; Eisele, S.; Riemer, D. D. *J. Geophys. Res.* **2003**, *108* (D20), 8794 (doi: 10.1029/2002JD003199).

(25) de Gouw, J. A.; Goldan, P. D.; Warneke, C.; Kuster, W. C.; Roberts, J. M.; Marchewka, M.; Bertman, S. B.; Pszenny, A. A. P.; Keene, W. C. *J. Geophys. Res.* **2003**, *108* (D21), 4682 (doi: 10.1029/2003JD003863).

(26) Goldan, P. D.; Kuster, W. C.; Williams, E.; Murphy, P. C.; Fehsenfeld, F. C.; Meagher, J. *J. Geophys. Res.* **2004**, *109*, D21309 (doi: 10.1029/2003JD004455).

Table 1. Suite of 98 Gases Measured with the Cryogen-Free GC System on Appledore Island

Methyl Halides	OVOCs	Alkanes	Alkenes
CH_3Cl	acetaldehyde	propane	propene
CH_3Br	propanal	isobutane	*trans*-2-butene
CH_3I	benzaldehyde	*n*-butane	*cis*-2-butene
	methanol	2,2-dimethylpropane	1-butene
CFCs	ethanol	cyclopentane	isobutene
CFC-12	l-propanol	isopentane	1-pentene
CFC-11	2-propanol	*n*-pentane	*trans*-2-pentene
CFC-113	1-butanol	2,2-dimethylbutane	*cis*-2-pentene
CFC-114	2-butanol	2,3-dimethylbutane	1-hexene
	acetone	2-methylpentane	
Solvents	methacrolein	3-methylpentane	Aromatics
CH_2Cl_2	methyl vinyl ketone	cyclohexane	benzene
$CHCl_3$	methyl ethyl ketone	methylcyclohexane	toluene
CH_3CCl_3		*n*-hexane	ethylbenzene
CCl_4	Sulfur Gases	*n*-heptane	*m*+*p*-xylene
C_2HCl_3	OCS	*n*-octane	*o*-xylene
C_2Cl_4	DMS	*n*-nonane	styrene
	CS_2	*n*-decane	isopropylbenzene
Mixed Halocarbons			*n*-propylbenzene
CH_2BrCl	Alkyl Nitrates	Biogenic NMHCs	*p*-ethyltoluene
$CHBrCl_2$	methyl nitrate	isoprene	*m*-ethyltoluene
$CHClBr_2$	ethyl nitrate	α-pinene	*o*-ethyltoluene
CH_2Br_2	isopropyl nitrate	*β*-pinene	1,3,5-trimethylbenzene
$CHBr_3$	*n*-propyl nitrate	camphene	1,2,4-trimethylbenzene
C_2H_5I	2-butyl nitrate	myrcene	1,2,3-trimethylbenzene
CH_2ClI	*n*-butyl nitrate	3-carene	1,2-diethylbenzene
CH_2BrI	3-pentyl nitrate	limonene	1,3-diethylbenzene
CH_2I_2	2-pentyl nitrate	*γ*-terpinene	1,4-diethylbenzene

five events in Figure 1 correspond to the eight different software states.

Splitter Box. At the splitter box, to alleviate the need for cryofocusing, a 3-m piece of 0.18-mm-i.d. deactivated fused silica was used to help sharpen the early-eluting peaks on all channels of the system. The sample was then reproducibly split into four streams at a 1-to-4-port manifold (Valco Instruments, $^1/_{16}$-in. manifold 1−4 ports). For three of the outlet ports, 0.74-mm Silonite tubing was used to connect the carrier flow from the manifold to each separation column. At the fourth outlet port, a 2-m piece of 0.18-mm-i.d. fused silica was connected to the manifold, which was then connected to the 0.74-mm transfer line to restrict the flow to the wide-bore (0.53-mm i.d.) CP-$A1_2O_3$/Na_2SO_4 PLOT column (Varian Inc., Walnut Creek, CA). Each of the four substreams fed a separate GC separation column housed in a single Shimadzu GC-17A gas chromatograph (Shimadzu Scientific, Columbia, MD) and was connected to an individual detector (Figure 2).

Gas Chromatography. A single Shimadzu GC-17A gas chromatograph housed the four separation columns and was temperature programmed as follows: the initial temperature was 35 °C for 3 min, the oven was ramped at 10 °C min^{-1} to 200 °C for 5 min. The suite of gases measured with the system is listed in Table 1. One 50 m × 0.53 mm i.d., 10-μm film thickness CP-$A1_2O_3$/Na_2SO_4 PLOT column, one 60 m × 0.25 mm i.d., 1-μm film thickness OV-1701 column (Ohio Valley Specialty Chemical, Marietta, OH), one 60 m × 0.32 mm i.d., 1.0-μm film thickness VF-5ms column (Varian Inc.), and one 60 m × 0.25 mm i.d., 1.4-μm film thickness OV-624 column (Ohio Valley Specialty Chemical) are used for trace gas separation. The OV-1701 column was plumbed into the ECD and was used for measuring halocarbons and alkyl nitrates. The PLOT and VF-5ms columns were connected to the FIDs and were used for the C_3−C_7 and C_5−C_{10} NMHC measurements, respectively. The OV-624 column provided separation for the Shimadzu QP-5050A MS, which was used primarily for OVOC analysis but also provided duplicate measurements of various halocarbons and NMHCs. For the GC/MS, electron impact mode was used for sample ionization along with single ion monitoring. At 25 °C, the main carrier flow and split was as follows: 48.6% (10.4 cm^3 min^{-1}) was directed to the PLOT/FID, 24.3% (5.2 cm^3 min^{-1}) to the VF-5ms/FID, 14.0% (3.0 cm^3 min^{-1}) to the OV-624/MS, and 13.1% (2.8 cm^3 min^{-1}) to the OV-1701 ECD.

For the MS channel, a secondary carrier was required to maintain high sensitivity, which could not be achieved otherwise since the main carrier flow rate through each capillary column was faster than optimal. However, little efficiency was lost in the resolving power of each column connected to the FIDs or ECD at these flow rates. A four-port switching valve (GCV) with one port capped off was placed in line for the transfer line feeding the MS channel and used to control the secondary carrier flow (Figure 2). In position A, the carrier flow passed through the switching valve and transfer line, allowing for the transfer of analytes to the separation column while the secondary carrier (also UHP helium), which was set at a flow rate of 1.5 cm^3 min^{-1} using a mass flow controller (MKS, Andover, MA), was directed to a dead end flow path. After the sample was injected for 1 min, the secondary carrier four-port switching valve was actuated to direct the main carrier to the dead end flow path while the secondary carrier flowed to the mass spectrometer. Within 1 min after injection, the sample aliquot was quantitatively split before peaks had eluted on any channel. The resulting slight increase in carrier flow through the columns to the FIDs and ECD was not detectable. Furthermore, since the first peak does not elute on the MS channel until ~2 min after the injection, the mass spectrometer was able to pump from 3.0×10^{-2} Pa down to 7.0×10^{-3} Pa, significantly increasing the sensitivity. Three minutes after injection, the SSV was moved from position 1 (dead end) to position 3 (UHP helium), and the

SV for the sample enrichment loop was switched back to position A (trap). At this time, the water management and sample enrichment loops were both heated to 100 °C and flushed with UHP helium for 5 min by opening valve 3. After the helium flush, the SSV was moved back to position 1 (dead end), valve 3 was closed, and the dewars containing the loops began cooling to their initial set points.

Makeup Gases. For each of the FIDs, UHP hydrogen and zero air from a catalytic converter/zero-air generator was used. An activated charcoal/molecular sieve (13X) trap was used for the UHP hydrogen to further remove impurities from the gas stream. The hydrogen flow rate to the FIDs was 35 cm^3 min^{-1}, and the zero-air flow rate was 340 cm^3 min^{-1}. Because a zero-air generator was used, a continuous supply was delivered to the FIDs without the need to change cylinders during operation of the system over multimonth-long periods. This helped to alleviate changes in sensitivity associated with variations in cylinders of compressed zero air.

UHP nitrogen was used as the makeup gas for the ECD and FIDs. Activated charcoal/molecular sieve (13X) traps were used on all delivery lines. A 40 cm^3 min^{-1} flow to the ECD provided optimum detector sensitivity. At higher flow rates, the sensitivity decreased, particularly for the alkyl nitrates. At lower flow rates, the baseline noise increased significantly. The nitrogen makeup flow rate to the FIDs was also 40 cm^3 min^{-1}. The sensitivity of the FID plateaued for nitrogen makeup flows between 30 and 47 cm^3 min^{-1}. The two FIDs, one ECD, and mass spectrometer were all operated at 250 °C, as this yielded the best sensitivity for the largest number of compounds for each detector.

Calibration. Whole air standards purchased from D. Blake at the University of California, Irvine (UCI) were analyzed every 10th run in a manner that was identical to ambient sampling. The NMHC calibration scale of the UCI standards has been rigorously evaluated as part of the Nonmethane Hydrocarbon Intercomparison Experiment (NOMHICE) sponsored by the National Center for Atmospheric Research (NCAR).[22] Overall, there was excellent agreement between the calibration scales of UCI and NCAR for all five tasks of NOMHICE.[22,27] Additionally, three different cylinders containing synthetic mixes (Apel-Riemer Environmental, Inc., Denver, CO) were used for the OVOC calibrations. These same three synthetic standards were also used for the PTR-MS calibrations during the summer field campaign and were diluted to atmospheric mixing ratios (ppbv to pptv levels) using whole air that had passed through a catalytic converter (0.5% Pd on alumina at 425 °C) to scrub the OVOCs and maintain conditions similar to the ambient air samples. The measurement precision for each of the halocarbons, hydrocarbons, alkyl nitrates, and OVOCs ranged from 0.3 to 15%.

The measurement precision for selected OVOCs in the two whole air standards (DC 1 and standard A) that were analyzed every 10th run is summarized in Table 2. The excellent precision achieved for these OVOCs gives us confidence both in the reliability of whole air OVOC standards during this time period and in the system's overall performance.

Table 2. Measurement Precision of Selected OVOCs from Two Different Whole Air Working Standards, DC1 and Standard A, Analyzed on Appledore Island

	acetaldehyde	methanol	acetone
DC 1			
ppbv	1.65	0.92	0.84
StDev	0.07	0.03	0.05
% RSD	4.5	3.6	6.2
standard A			
ppbv	0.91	1.03	1.26
StDev	0.01	0.03	0.05
% RSD	0.8	2.7	4.1

RESULTS

Ambient Air Performance Tests. The GC system, herein referred to as the MMR-GC, was located on the top floor of a ~20-m-tall World War II-era coastal surveillance tower that is now part of the Cornell University/UNH Shoals Marine Laboratory. The site is located on Appledore Island ~10 km off the New Hampshire coastline in the Gulf of Maine. This site is frequently influenced by pollutant emissions from the urban/industrial eastern United States.[28] During summer 2004, this site was equipped with atmospheric chemistry instrumentation as part of the International Consortium for Atmospheric Research on Transport and Transformation (see http://www.al.noaa.gov/ICARTT/), the most extensive air quality field campaign conducted to date.

For our VOC measurements, ambient air was drawn from 4 m above the roof of the tower using a 6 cm × 0.635 cm o.d. Silonite-coated stainless steel line. To keep the line equilibrated, flow was maintained continuously at a rate of ~15 L min^{-1} using a metal bellows pump (MB-158, Senior Flexionics, Sharon, MA) and delivered at a pressure of 20 psig to the analytical system. Laboratory tests using ambient air and calibrated standards were conducted to ensure that the compounds listed in Table 1 were not affected by passing the air stream through the metal bellows pump. The MMR-GC collected a 1500-cm^3 aliquot of ambient air representing a 7.5-min integrated sample every 40 min. For the PTR-MS VOC measurements, the instrument continuously stepped through a series of 30 masses; 6 masses were used for diagnostic purposes while 24 masses corresponded to the VOCs of interest. The dwell time for each of the 24 masses was 20 s during the ICARTT campaign, yielding a total measurement cycle of ~10 min. Aliquots of ambient air were collected in canisters once per hour over a 5-min sampling period using a metal bellows pump to pressurize the sample canisters to 40 psig.

To demonstrate the capabilities of this novel trace gas analytical system, results for these simultaneous measurements of ambient air are compared from the MMR-GC system, the PTR-MS, and whole air canister samples analyzed at UNH as described previously. Overall, excellent agreement was observed between the three measurement techniques for the majority of compounds.

For the OVOC measurements, we first compared the MMR-GC system results to that of the PTR-MS, which is now a routinely used technique for measurements of certain atmospheric OVOCs.[25] Time series of plots are shown in Figure 3 for (a) acetone, (b) methanol, and (c) acetaldehyde atmospheric mixing ratios as determined using the MMR-GC and PTR-MS analytical systems. Overall, both sets of measurements tracked each other well in

(27) Sive, B. C. Ph.D. Thesis, University of California, Irvine, 1998.

(28) Mao, H.; Talbot, R. *J. Geophys. Res.* **2004**, *109*, (D20305) (doi: 10.1029/2004JD004850).

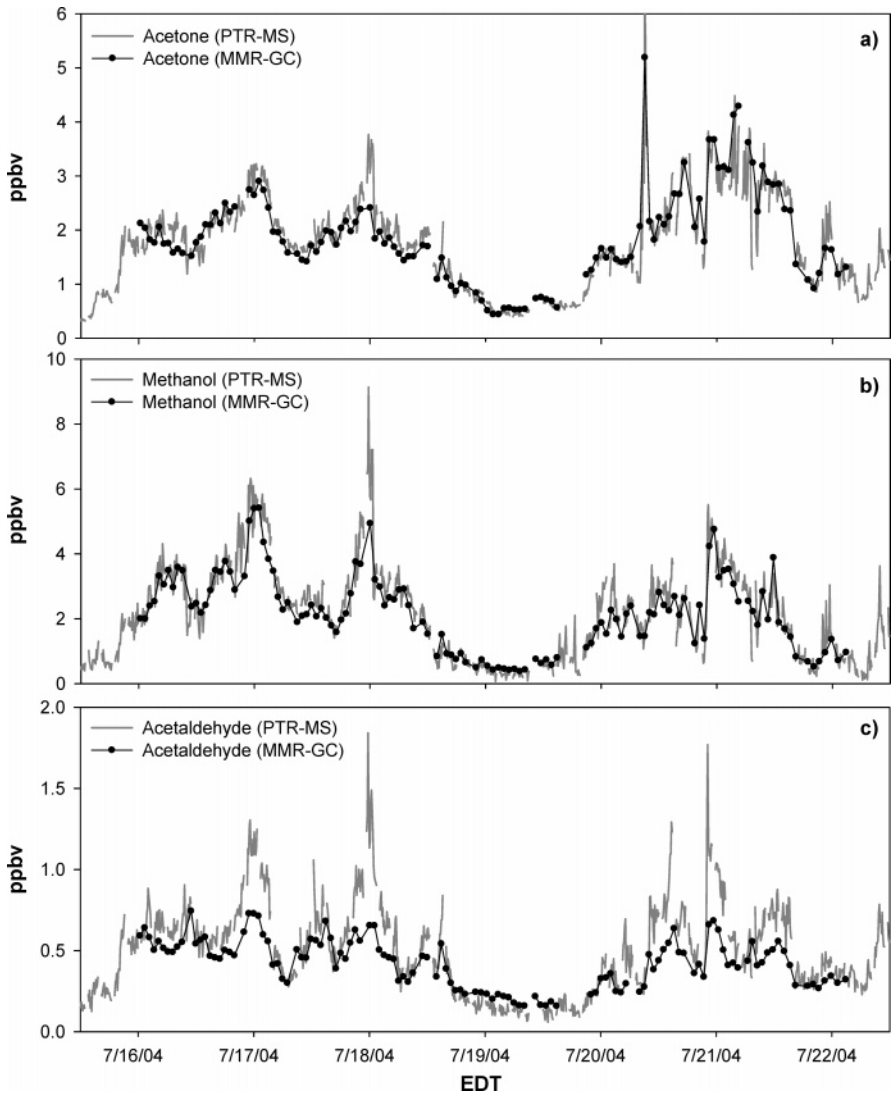

Figure 3. Time series plots of (a) acetone, (b) methanol, and (c) acetaldehyde for the MMR-GC and PTR-MS on Appledore Island, July 16−22, 2004.

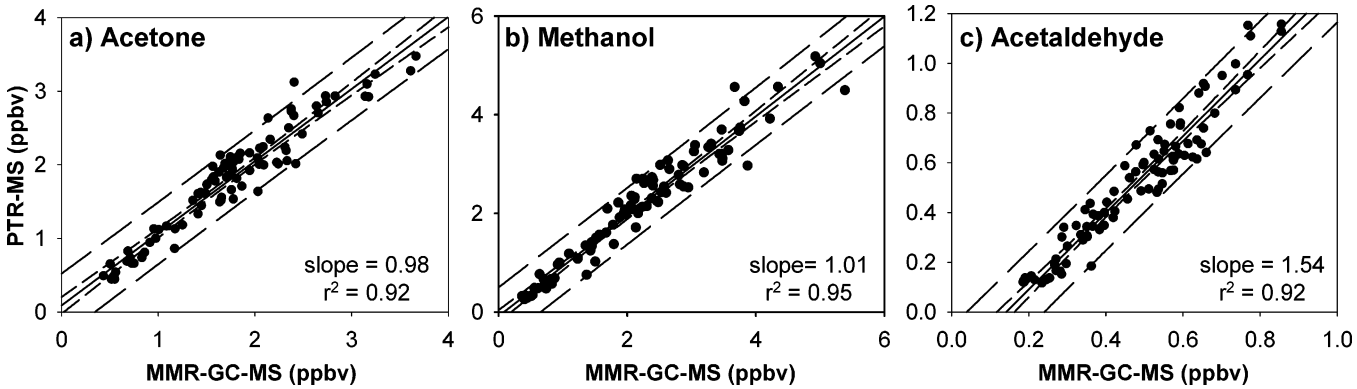

Figure 4. Correlations of ambient mixing ratios of (a) acetone, (b) methanol, and (c) acetaldehyde determined with the PTR-MS versus MMR-GC on Appledore Island, July 16−22, 2004. The best fit line from the linear regression is represented by the innermost solid line. The inner dashed lines represent the 95% confidence interval for the best fit line. The outer dashed lines represent the 95% prediction interval for the measurements.

depicting small- and large-scale features. The absolute mixing ratios also are in good agreement, with both yielding similar mean and median values. The largest differences in OVOCs between the two systems occurred for acetaldehyde. Although mixing ratios measured by the two methods are in agreement and both systems tracked each other reasonably well, there are discrepancies during events where the PTR-MS values are higher than those from the MMR-GC system. These disagreements are also evident in correlation plots of the PTR-MS versus MMR-GC determined mixing ratios for (a) acetone, (b) methanol, and (c)

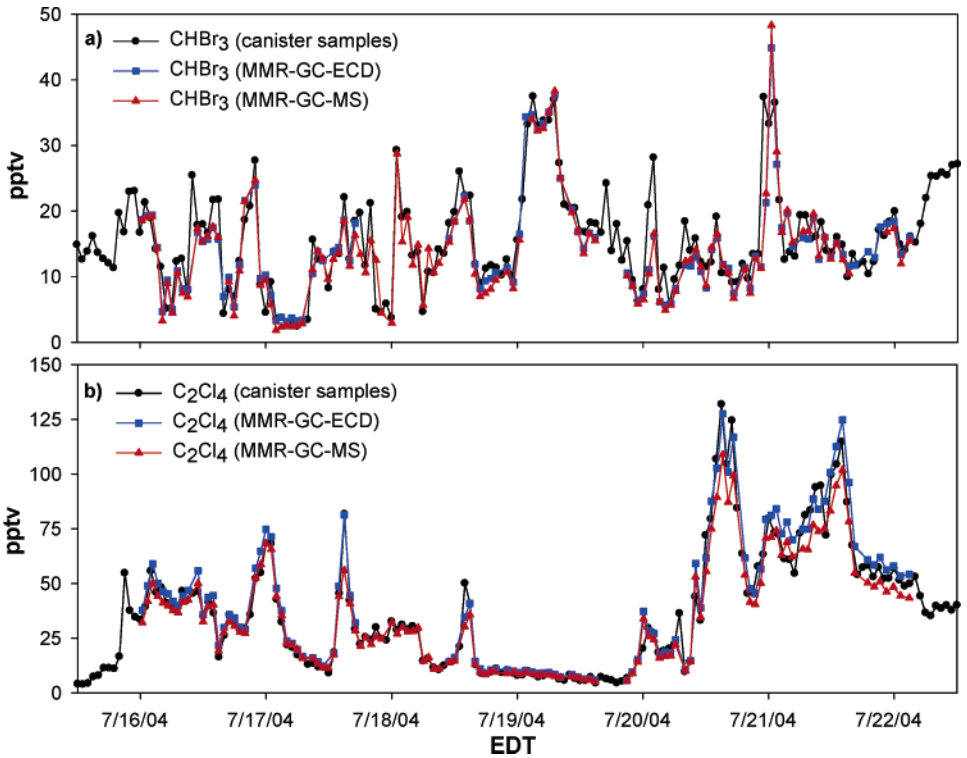

Figure 5. Time series plots of (a) $CHBr_3$ and (b) C_2Cl_4 for the real-time MMR-GC and canister samples collected on Appledore Island, July 16−22, 2004. Individual measurements for the ECD and MS are shown separately for the MMR-GC system.

acetaldehyde (Figure 4). Good correlations existed overall for all three compounds (i.e., r^2 values ranged from 0.92 to 0.95), with the linear regression yielding slopes of 0.98 and 1.01 for acetone and methanol, respectively. Although a good correlation exists for acetaldehyde ($r^2 = 0.92$), the linear regression yielded a slope of 1.54, indicating discrepancies between these techniques. These discrepancies could be due to confounding production of mass 45 ion fragments, the mass used for acetaldehyde quantification, in the PTR-MS instrument during the sampling of polluted air masses with high ozone (>80 ppbv). Acetaldehyde artifacts were observed in a PTR-MS instrument flown near the tropopause during a stratospheric intrusion event that had ozone mixing ratios as high as 300 ppbv.[26]

Conversely, the disagreement could be related to losses or destruction of acetaldehyde in the MMR-GC system during either the sampling or the analysis phases, even though we have taken extreme precautions to avoid such problems. Aldehydes are notoriously difficult to measure reliably, with a positive artifact commonly being related to contamination or production in the measurement system. For example, Apel et al.[24] have reported ozone artifacts associated with sampling and concentrating compounds such as acetaldehyde. They attributed these positive artifact problems to the sampling pump (KNF Teflon diaphragm pump) and rotor material in the Valco valves.[24] Other investigators have subsequently conducted similar types of experiments with results[25,26] that corroborate the Apel et al.[24] findings. For example, Goldan et al.[26] found that the most abundantly produced artifacts during ozone exposure tests have always been acetaldehyde and *n*-hexanal with lesser amounts of all other straight-chain aldehydes and still smaller amounts of branched aldehydes. To minimize aldehyde artifacts associated with sampling air masses with high ozone, we have found that baking the Valcon E rotor at 200 °C for 12 h in humidified air greatly reduces this problem (E. Apel, NCAR and D. Riemer, University of Miami, personal communication, 2003). Nonetheless, further investigation of both of analytical systems is clearly needed in the case of acetaldehyde, but it is beyond the scope of this paper.

Comparison of results obtained with the MMR-GC system to those of traditional whole air canister samples demonstrates the diversity of compounds this new system is capable of accurately quantifying. To illustrate this, a time series is shown in Figure 5 for two different halocarbons, (a) bromoform ($CHBr_3$), a marine-derived compound, and (b) tetrachloroethene (C_2Cl_4), a tracer of anthropogenic activity. With the MMR-GC system, these gases were measured using detection by the ECD and MS channels. These data are presented here as two individual measurements to demonstrate the reproducibly and quantitative four-way splitting of each air sample. There was excellent quantitative agreement between each detector of the MMR-GC system and the canister samples. Both the real-time and canister techniques captured the high variability of the marine-derived compound $CHBr_3$ (Figure 5a). In contrast to $CHBr_3$, the urban tracer C_2Cl_4 exhibited a much different time series structure (Figure 5b), with both techniques accurately capturing the major features. In the case of $CHBr_3$, the linear regression between the two data sets had a slope of 0.98 with $r^2 = 0.88$ for the MS channel and 0.96 with $r^2 = 0.85$ for the ECD channel. Equally comparable results were obtained for C_2Cl_4, where the slope for the MS channel was 0.94 with $r^2 = 0.96$ and that for the ECD was 0.99 with $r^2 = 0.97$.

Finally, good agreement was also observed for the alkyl nitrates and a large suite of NMHCs. The alkyl nitrates were measured on the ECD channel of the real-time MMR-GC, with an example of the agreement illustrated in Figure 6 for isopropyl nitrate and

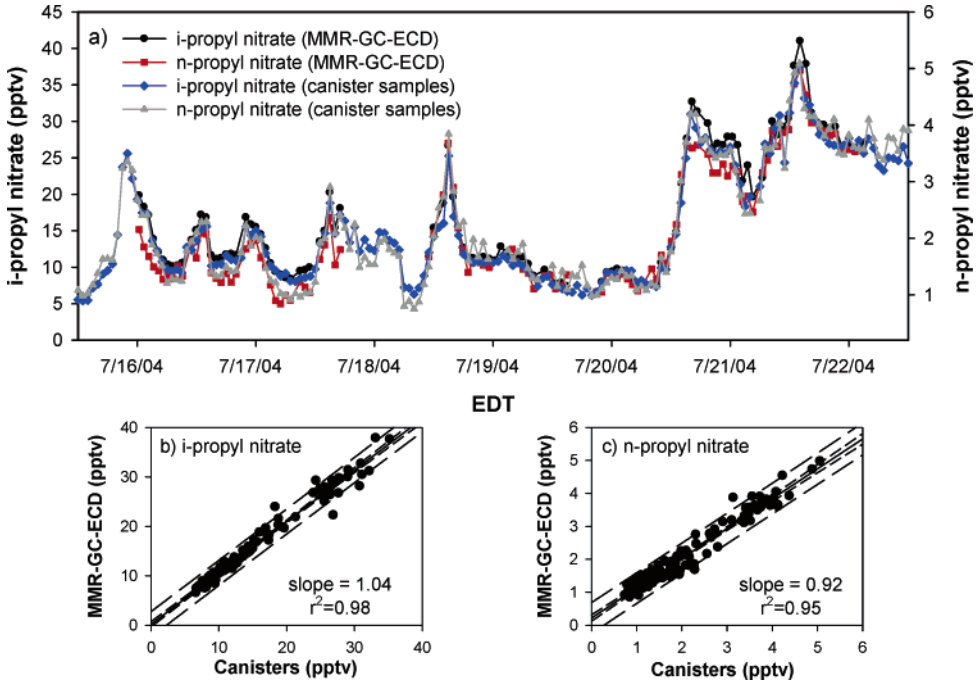

Figure 6. Time series plot of (a) isopropyl nitrate and *n*-propyl nitrate for the real-time MMR-GC and canister samples collected on Appledore Island, July 16−22, 2004. The correlation of (b) isopropyl nitrate and (c) *n*-propyl nitrate between the canister samples and the MMR-GC. The best fit line from the linear regression is represented by the innermost solid line. The inner dashed lines represent the 95% confidence interval for the best fit line while the outer dashed lines represent the 95% prediction interval for the measurements.

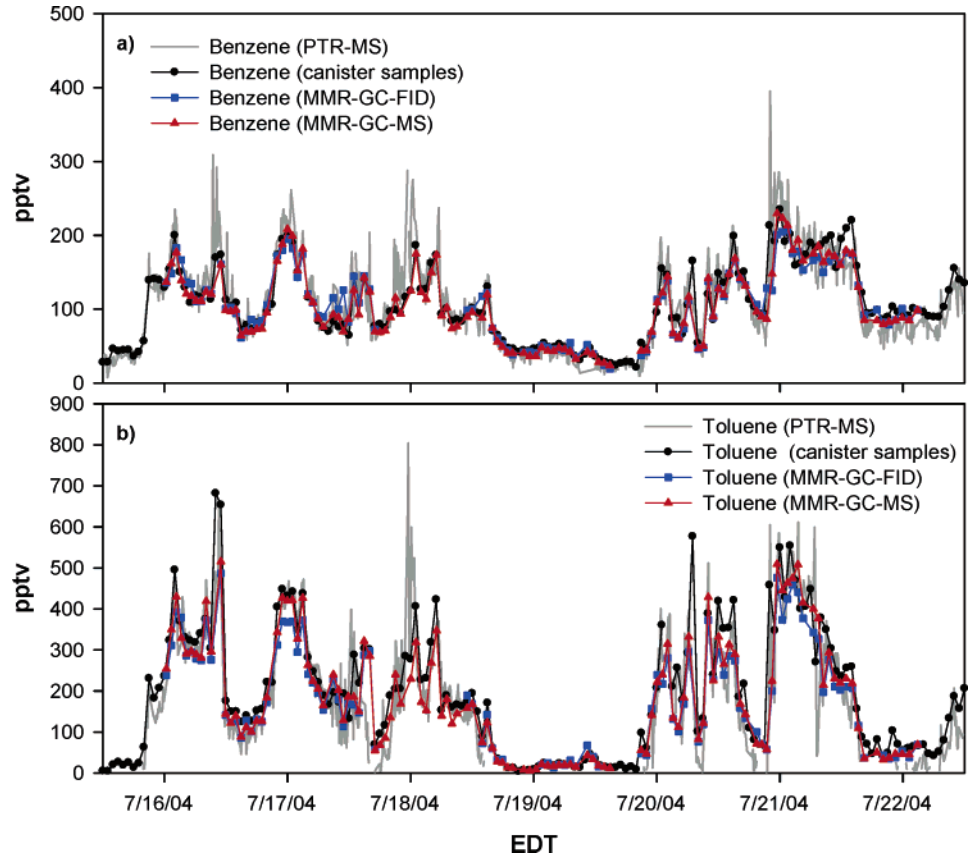

Figure 7. Time series plot of (a) benzene and (b) toluene for the real-time PTR-MS, MMR-GC, and canister samples collected on Appledore Island, July 16−22, 2004. Individual measurements for the FID and MS are shown separately for the MMR-GC system.

n-propyl nitrate with the canister samples. For the NMHCs, there was good agreement for aromatic hydrocarbons, which were measured by all techniques (PTR-MS, MMR-GC, and canister samples). In this case, we show results for benzene and toluene in Figure 7a and b, respectively, using the FID and MS channels as independent measurements.

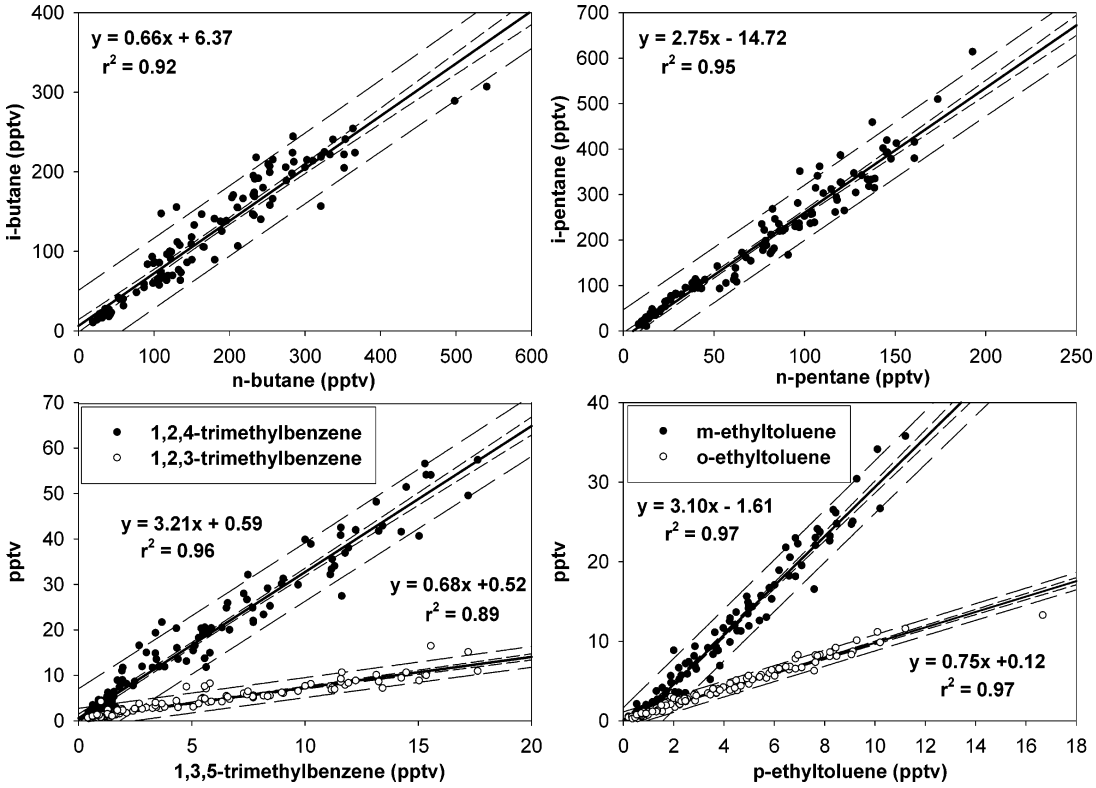

Figure 8. MMR-GC correlations of (a) isobutane and *n*-butane, (b) isopentane and *n*-pentane, (c) 1,2,4- and 1,2,3-trimethylbenzene versus 1,3,5-trimethylbenzene, and (d) *m*-ethyltoluene and *o*-ethyltoluene versus *p*-ethyltoluene on Appledore Island, July 16−22, 2004. The best fit line from the linear regression is represented by the innermost solid line. The innermost dashed lines represent the 95% confidence interval for the best fit line. The outer dashed lines represent the 95% prediction interval for the measurements.

Correlations of several NMHCs were examined to further demonstrate the quality of the measurements performed with the MMR-GC system. Robust correlations of these gases are expected since the selected pairs have common anthropogenic sources. Figure 8 shows the correlations of (a) isobutane and *n*-butane, (b) isopentane and *n*-pentane, (c) 1,2,4- and 1,2,3-trimethylbenzene versus 1,3,5-trimethylbenzene, and (d) *m*-ethyltoluene and *o*-ethyltoluene versus *p*-ethyltoluene. These gases exhibited correlations with $r^2 > 0.92$ over 1 order of magnitude change in ambient mixing ratios. It is worth noting that the strong correlations persisted even at sub-pptv mixing ratios, highlighting the excellent performance of the automated MMR-GC system.

CONCLUSIONS

Overall, the new MMR-GC system developed by our research group offers extremely high sensitivities and selectivity for measuring a large suite of atmospheric VOCs. Comparison of results obtained from this real-time system with well-established techniques clearly demonstrates its ability to provide high-quality measurements, even at sub-pptv mixing ratios. A major inherent advantage of the MMR-GC system is the capability to make accurate and precise VOC measurements in remote locations where cryogens, such as liquid nitrogen, are not readily available. Moreover, the system eliminates the use of solid adsorbents for the concentration of air samples, a method known to be prone to artifacts. The system operated autonomously for ~5 months prior to deployment on Appledore Island and, more recently, for 6 months in the laboratory demonstrating its durability and reliability. One aspect of this multichannel system that has not yet been exploited is its versatility for measuring a wide variety of compounds in other applications.

ACKNOWLEDGMENT

Financial support for this work was provided through the Office of Oceanic and Atmospheric Research at the National Oceanic and Atmospheric Administration under grants NA17RP2632 and NA03OAR4600122. Additional support for the research conducted on Appledore Island was provided by the National Science Foundation through grant 0401622. This paper is contribution number 122 to the Shoals Marine Laboratory. We thank the Shoals Marine Laboratory and the Isles of Shoals Steamship Company for their assistance and support during the field campaign. Finally, we thank Lissa Ducharme and the UCI group, especially Dr. Donald R. Blake and Mr. Kevin Gervais.

Received for review April 12, 2005. Accepted July 21, 2005.

AC0506231